

Categorization by a Three-state Attractor Neural Network

D.R.C. Dominguez ¹ and D. Bollé ²⁽¹⁾

Instituut voor Theoretische Fysica, K.U. Leuven
B-3001 Leuven, Belgium

Abstract

The categorization properties of an attractor network of three-state neurons which infers three-state concepts from examples are studied. The evolution equations governing the parallel dynamics at zero temperature for the overlap between the state of the network and the examples, the state of the network and the concepts as well as the neuron activity are discussed in the limit of extreme dilution. A transition from a retrieval region to a categorization region is found when the number of examples or their correlations are increased. If the pattern activity is small enough, the examples (concepts) are very well retrieved (categorized) for an appropriate choice of the zero-activity threshold of the neurons.

¹e-mail:david@tfdec1.fys.kuleuven.ac.be

²e-mail: desire.bolle@fys.kuleuven.ac.be

⁽¹⁾ Also at Interdisciplinair Centrum voor Neurale Netwerken, K.U.Leuven

1. Introduction

Some years ago a minimal modification of the Hopfield model has been suggested such that categorization of patterns emerges naturally from an encoding stage structured in layers [1]. The network is spatially homogenous in the sense that the synaptic couplings between all neurons are of the same type, but the patterns are hierarchically ordered, meaning that patterns belonging to the same group are strongly correlated while patterns sitting in distinct groups are only weakly correlated. Related models of this type have been examined in [2]-[5]. These models lead to the appearance of stable states besides those corresponding to the original patterns, e.g., the ancestors of the categories to which those patterns belong.

Shortly after, a simple Hebbian rule has been proposed in order to study the performance of a network in learning an extensive number of ancestor patterns in such an hierarchical ordering, given that the learning takes place with groups of a finite number of (correlated) patterns situated on a lower level of the hierarchical tree [6]. In other words the problem of categorizing examples (i.e. the correlated patterns) into classes defined by concepts (i.e. the ancestors) is studied. It turns out that such a network loses its ability to retrieve the examples when a critical number of them is presented during the learning stage, but it then gets the ability to categorize the concepts [6]-[10].

This categorization property occurring in fact through learning from examples is thus a particular kind of generalization. Generalization has been a topic of intensive research in recent years. (For recent reviews emphasizing different aspects see [11]-[14].)

Recently, models with multi-state and analogue neurons have been introduced in the study of categorization problems [15, 16]. By using analogue neurons [15], less (binary) examples are needed in order to start categorization. However, the generalization error, i.e., the Hamming distance between the microscopic state of the network and the (binary) concepts is larger than in the corresponding two-state model. A further improvement is obtained by using low-activity examples, from which (binary) full-activity concepts can be inferred, even if the number of examples is small [16]. This must be due to the fact that mixture states of patterns can be inherently stable, allowing the network to ultimately form higher activity patterns out of smaller ones, just like happens in the retrieval regime for both highly diluted [17] and fully connected three-state networks [18].

In this paper we extend these models by allowing the concepts themselves to be three-state. Furthermore, we do not require full symmetry of the retrieval overlaps of the examples. At the same time we study the conditions characterizing the transition from the retrieval phase to the categorization phase. These problems are considered in an asymmetrically diluted network with a Hebbian type learning rule because, as is standard knowledge by now, its parallel dynamics can be solved exactly [19]. The following main results are found. When the number of examples (per concept) presented to the network is too small or their correlations are too weak, it behaves as a retrieval (of examples) device. When one of these parameters attains a large enough value the network starts categorizing. The latter behavior can be considerably improved by appropriately choosing the zero-activity threshold of the neurons. Compared with the categorization properties of the binary concept model [16], we find that the categorization error is smaller and that a greater number of concepts can be categorized.

The rest of this paper is organized as follows. In Section 2 we introduce the model and the relevant Hamming distances as macroscopic measures for the retrieval and categorization quality of the model. Section 3 solves the parallel dynamics leading to evolution equations for the retrieval overlap, the categorization overlap and the neuron activity. In Section 4 we study the retrieval and categorization phases as a function of the zero-activity threshold of the neurons, the number of concepts, the number of examples per concept, their correlations and their activity. Finally, Section 5 presents some concluding remarks.

2. The model

Consider a network of N three-state neurons. At time t and zero temperature the neurons $\{\sigma_{i,t}\}$ are updated in parallel according to the rule

$$\sigma_{i,t+1} = F_{\theta}(h_{i,t}), \quad i = 1, \dots, N \quad (1)$$

$$h_{i,t} = \sum_{j(\neq i)} J_{ij} \sigma_{j,t}, \quad (2)$$

where $h_{i,t}$ is the local field of neuron i at time t . The input-output relation F_{θ} is, in general, a monotonous function and will later on be chosen as the

three-state step-like function

$$F_\theta(x) = \begin{cases} \text{sign}(x) & \text{if } |x| > \theta \\ 0 & \text{if } |x| < \theta \end{cases} \quad (3)$$

where θ is the zero-activity threshold parameter of the neurons. The synaptic couplings J_{ij} are determined through the learning of s three-state examples, $\eta_i^{\mu\rho} \in \{0, \pm 1\}$, $\mu = 1, \dots, p$, $\rho = 1, \dots, s$, of p three-state concepts, $\xi_i^\mu \in \{0, \pm 1\}$. The examples have zero mean and variance $A = 1/N \sum_i (\eta_i^{\mu\rho})^2$, which is a measure for their activity. The concepts ξ_i^μ are chosen to be independent identically distributed random variables (i.i.d.r.v.) with mean zero and activity equal to the activity A of the examples. The following Hebbian-type algorithm is taken

$$J_{ij} = \frac{1}{NA} \sum_{\mu=1}^p \sum_{\rho=1}^s \eta_i^{\mu\rho} \eta_j^{\mu\rho}. \quad (4)$$

Furthermore, each set of examples $\{\eta_i^{\mu\rho}\}_{\rho=1}^s$ at site $i = 1, \dots, N$ is built from the concept ξ_i^μ through the following process

$$\eta_i^{\mu\rho} = \xi_i^\mu \lambda_i^{\mu\rho}, \quad \lambda_i^{\mu\rho} \in \{\pm 1\}. \quad (5)$$

The variables $\lambda_i^{\mu\rho}$ are also taken to be i.i.d.r.v. with a bias towards the value +1 such that they are given by the probability distribution

$$p(\lambda_i^{\mu\rho}) = b_+ \delta(\lambda_i^{\mu\rho} - 1) + b_- \delta(\lambda_i^{\mu\rho} + 1), \quad (6)$$

with $b_\pm = (1 \pm b)/2$. The parameter b describes the correlation between the stored example $\eta_i^{\mu\rho}$ and its concept ξ_j^μ , viz. $\langle \eta_i^{\mu\rho} \xi_j^\mu \rangle = bA\delta_{ij}$, and the correlation between two different examples of the same concept $\langle \eta_i^{\mu\rho} \eta_j^{\mu\sigma} \rangle = b^2 A \delta_{ij}$.

At this point we remark that, on the one hand we recover the binary categorization model [6] by setting $A = 1$ and $\theta = 0$. On the other hand, the standard three-state neuron model [17] is obtained by taking the number of examples in Eq.(4) to be 1 and the correlation $b = 1$.

In order to measure the quality of retrieval of the examples we introduce the Hamming distance between the stored example and the microscopic state of the network [20]

$$D_t^{\mu\rho} = \frac{1}{N} \sum_i [\eta_i^{\mu\rho} - \sigma_{i,t}]^2 = A - 2A m_{N,t}^{\mu\rho} + Q_{N,t}. \quad (7)$$

This defines the retrieval overlap between the microscopic state of the network and the ρ th example of the μ th concept

$$m_{N,t}^{\mu\rho} = \frac{1}{NA} \sum_i \eta_i^{\mu\rho} \sigma_{i,t}. \quad (8)$$

These are normalized order parameters within the interval $[-1, 1]$, which attain the maximal value $m_N^{\mu\rho} = 1$ whenever $\sigma_i = \eta_i^{\mu\rho}$ (recall Eq.(5)). Furthermore, also the neuron activity is introduced

$$Q_{N,t} = \frac{1}{N} \sum_i |\sigma_{i,t}|^2. \quad (9)$$

The task of categorization is successful when the distance between the microscopic state of the network and the concept ξ_i^μ , defined as

$$E_t^\mu = \frac{1}{N} \sum_i [\xi_i^\mu - \sigma_{i,t}]^2 = A - 2AM_{N,t}^\mu + Q_{N,t} \quad (10)$$

becomes small after some time t . As explained in the introduction the quantity E_t^μ can be considered as the generalization error in this context. (We refer to the refs. ([11]-[14]) for a comparison with definitions of the generalization error in related contexts of learning from examples.) In obtaining the second equality of Eq. 10 we have used the fact that the activity of the concepts and the examples are taken to be equal. Furthermore, the overlap between the microscopic state of the network and the concept is defined as

$$M_{N,t}^\mu = \frac{1}{NA} \sum_i \xi_i^\mu \sigma_{i,t}. \quad (11)$$

We now want to consider an extremely diluted asymmetric version of this model in which each neuron is connected, on average, with C other neurons through the synaptic couplings (see expression (4))

$$J_{ij}(C) = C_{ij} \frac{N}{C} J_{ij} = \frac{C_{ij}}{CA} \sum_{\mu=1}^p \sum_{\rho=1}^s \eta_i^{\mu\rho} \eta_j^{\mu\rho}. \quad (12)$$

Here, the $C_{ij} \in \{0, 1\}$ are i.i.d.r.v. with probability $\Pr\{C_{ij} = 1\} = C/N, C > 0$. These C_{ij} are highly asymmetric such that in the limit of extreme dilution, $C \ll \log N$, the architecture of the network gets the structure of a directed

tree and the neurons are uncorrelated for almost all sites i . This allows an exact solution of the parallel dynamics [19].

In the next section we discuss this solution by writing down the evolution equations for the retrieval overlap, the neuron activity and the categorization overlap.

3. The diluted dynamics

Because we are interested in both the retrieval and categorization properties of the network, we take an initial configuration correlated with only one concept meaning that only the retrieval overlaps for the s examples of that given concept, say the first one, are macroscopic, i.e., of order $O(1)$ in the thermodynamic limit $N \rightarrow \infty$. In order to study the retrieval of a particular example we single out the component $\rho = 1$. We furthermore assume that all other components are the same i.e., $m_{N,t}^{1\rho} = m_{N,t}^{1s}$ for all $\rho > 1$. This property of the examples is called quasi-symmetry. It extends former work (e.g., [16]) where full symmetry of the examples has been assumed.

The dynamics of this model is then studied following standard methods involving a signal-to-noise analysis (see, e.g., [19], [20], [21]). At this point we recall that it is justified to first dilute the system by taking the limit $N \rightarrow \infty$ and second, in the diluted system, to apply the law of large numbers (LLN) and the central limit theorem (CLT) by taking the limit $C \rightarrow \infty$. Furthermore the retrieval overlaps have to be considered over the diluted structure and the loading α is defined by $p = \alpha C$. Finally, we know that because of the extremely diluted structure of the network the equations derived for the first time step are valid for any time step.

Splitting the local field (2) into a signal and noise part gives

$$h_{i,t} = \eta_i^{11} m_{C,t}^{11} + \sum_{\rho>1}^s \eta_i^{1\rho} m_{C,t}^{1\rho} + \sum_{\mu>1}^p \sum_{\rho}^s \eta_i^{\mu\rho} \sum_{j \neq i}^N \frac{C_{ij}}{CA} \eta_j^{\mu\rho} \sigma_{j,t} \quad (13)$$

with

$$m_{C,t}^{1\rho} = \sum_{j(\neq i)}^N \frac{C_{ij}}{CA} \eta_j^{1\rho} \sigma_{j,t}. \quad (14)$$

In the thermodynamic limit we then obtain in a standard way ([16], [19], [20], [21])

$$m_{t+1}^{11} = \langle \langle \langle \lambda^{11} F_{\theta}(\tilde{h}_t) \rangle_{\lambda^{11}} \rangle_{x_s} \rangle_{\omega_t} \quad (15)$$

$$m_{t+1}^{1s} = \langle \langle \langle x_s F_\theta(\tilde{h}_t) \rangle_{\lambda^{11}} \rangle_{x_s} \rangle_{\omega_t} \quad (16)$$

$$M_{t+1}^1 = \langle \langle \langle F_\theta(\tilde{h}_t) \rangle_{\lambda^{11}} \rangle_{x_s} \rangle_{\omega_t} \quad (17)$$

$$Q_{t+1} = A \langle \langle \langle [F_\theta(\tilde{h}_t)]^2 \rangle_{\lambda^{11}} \rangle_{x_s} \rangle_{\omega_t} + (1 - A) \langle [F_\theta(\omega_t)]^2 \rangle_{\omega_t}. \quad (18)$$

with

$$\tilde{h}_t \doteq \lambda_t^{11} m_t^{11} + (s - 1) x_s m_t^{1s} + \omega_t \quad (19)$$

$$\omega_t = [\alpha r Q_t]^{1/2} \mathcal{N}(0, 1). \quad (20)$$

Here \doteq indicates that this relation is valid in distribution, $x_s = \frac{1}{s-1} \sum_{\rho>1}^s \lambda^{1\rho}$, $r = s(1 + (s-1)b^4)$ and the quantity $\mathcal{N}(0, 1)$ is a Gaussian random variable with mean zero and variance unity. Furthermore, we have averaged already over ξ^1 . The brackets denote the further averages over both λ^{11} , x_s and over ω_t . We recall that the average over λ^{11} has to be done according to the distribution (6).

The first term in the expression (19) is the signal coming from the first example of the first concept, while the second term, recalling the assumed quasi-symmetry of the examples, represents the signal of the other examples of the first concept. It has a strength factor x_s . The third term is the noise caused by the examples of the $(p-1)$ residual non-condensed concepts.

These Eqs.(15)-(18) give a complete description of the dynamics for the retrieval of examples and the categorization of the concepts by the network we are considering for a general monotonous input-output function F_θ . Chosing F_θ to be the three-state function (3) we obtain the following explicit forms for the dynamics

$$m_{t+1}^{11} = \sum_{j=0}^{s-1} p_b(j) \{b_+ [\Psi_t^+(\Omega_+) + \Psi_t^-(\Omega_+)] - b_- [\Psi_t^+(\Omega_-) + \Psi_t^-(\Omega_-)]\} \quad (21)$$

$$m_{t+1}^{1s} = \sum_{j=0}^{s-1} p_b(j) \frac{2j - s + 1}{s - 1} \{b_+ [\Psi_t^+(\Omega_+) + \Psi_t^-(\Omega_+)] + b_- [\Psi_t^+(\Omega_-) + \Psi_t^-(\Omega_-)]\} \quad (22)$$

$$M_{t+1}^1 = \sum_{j=0}^{s-1} p_b(j) s \{b_+ [\Psi_t^+(\Omega_+) + \Psi_t^-(\Omega_+)] + b_- [\Psi_t^+(\Omega_-) + \Psi_t^-(\Omega_-)]\} \quad (23)$$

$$Q_{t+1} = 1 - A \sum_{j=0}^{s-1} p_b(j) \{b_+ [\Psi_t^+(\Omega_+) - \Psi_t^-(\Omega_+)] + b_- [\Psi_t^+(\Omega_-) - \Psi_t^-(\Omega_-)]\} - 2(1 - A) [\Psi_t^+(0)]. \quad (24)$$

Here

$$p_b(j) = \binom{s-1}{j} b_+^j b_-^{s-1-j}, \quad (25)$$

and

$$\Psi_t^\pm(\Omega_\pm) = \text{erf}\left(\frac{\Omega_\pm \pm \theta}{\sqrt{\alpha r Q_t}}\right), \quad \Omega_\pm = (2j - s + 1)m_t^{1s} \pm m_t^{11}, \quad (26)$$

where $\text{erf}(x) = \int_0^x dz e^{-z^2/2} / \sqrt{2\pi}$. In the case that we have many examples per concept we use for x_s defined before the Gaussian approximation $x_s \doteq b + z_s \sqrt{\frac{1-b^2}{s-1}}$ with $z_s = \mathcal{N}(0, 1)$ independent of ω_t .

4. Retrieval and categorization

We now discuss the structure of the retrieval and categorization dynamics which can be extracted by numerical solution of the fixed-point equations given by (21)-(24) (by leaving out the t -dependence).

Besides the zero solution Z determined by $m^{11} = M^1 = Q = 0$ it is necessary to distinguish among the following different types of solution: the retrieval solutions R defined by $m^{11} > M^1 > 0$ and $Q > 0$, the categorization solutions G defined by $0 < m^{11} < M^1$ and $Q > 0$ and the self-sustained activity [22] solutions S with $Q > 0$ but $m^{11} = M^1 = 0$. For the retrieval respectively categorization solution we impose the further condition $D < 0.1$ respectively $E < 0.1$. Hereby the numbers 0.1 are somewhat arbitrarily chosen but the idea is to guarantee a minimal retrieval respectively generalization quality of the network.

Since there are many parameters to be considered in the discussion of the numerical results we only show in Figs. 1-6 the properties of the network we believe to be typical and important.

Figure 1 shows the Hamming distance $D = D_\infty^{11}$, the generalization error $E = E_\infty^1$ and the neuron activity $Q = Q_\infty$ as a function of the correlation b . The other parameters are chosen as follows: the number of examples $s = 5$, the loading rate $\alpha = 0.01$, the activity A takes the values 1 (binary) in the upper part of the figure and 0.3 (three-state) in the lower part, and the zero-activity threshold θ is 0 (binary) in the left part of the figure and 0.5 (three-state) in the right part. For binary patterns it is seen that the use of three-state neurons does not affect the overall behaviour of the network. However, for three-state patterns both the retrieval and the categorization abilities are improved. The transition from a R phase to a G phase is clearly

present in all data. For a critical value of the correlation, b_c , there is a crossing between the D and E lines. Here we remark that in the case of three-state patterns ($A = 0.3$) and binary neurons ($\theta = 0$) the conditions for good retrieval and categorization behaviour of the full patterns are, of course, not satisfied. But as the curves indicate, e.g., one finds the best possible retrieval of the active sites ($D = 0.7$ for $b < b_c$). Furthermore, we also note the existence of a plateau for D in the case of three-state patterns and three-state neurons, where the Hamming distance is not small but it still satisfies $D < E$. Finally, in all cases there exists a minimal value for E meaning that the categorization is optimal for the corresponding network parameters. This does not always happen for $b = 1$, the reason being that although the neuron activity Q becomes high for large b , the pattern activity A may be so small that σ_i can not match ξ_i . This is in agreement with Eq.(10).

This behaviour is further illustrated in typical (θ, b) and (A, b) phase diagrams, Fig. 2 respectively Fig. 3, where the different phases corresponding to the solutions of the fixed-point equations described before are shown. We have divided the R -phase in two regions, one of them (R_+) referring to the region where D is almost zero, the other one (R_-) indicating the region where D has already jumped to the plateau seen in Fig. 1. The thin dashed line G_{opt} in the phase diagrams describes the optimal categorization. We remark the existence of two S -phases in Fig. 3, the first one separating the R - and G -phase, the second one occuring for large correlations b . The first indicates a region where b is already too large to have retrieval but still too small to allow categorization. The second describes the high neuron activity region for large b mentioned above.

In Fig. 4 we plot the behaviour of the network as a function of the zero-activity threshold θ for $A = 0.01$ and $s = 80$ examples per concept. On the left we show both the retrieval overlap m and the overlap with a concept M for $\alpha = 0.02$ and small correlations $b = 0.1$ such that a R -phase exists. For an appropriate choice of the threshold $m \approx 1$ while M becomes small. Thereby we note that although the concept storage seems to be rather small ($\alpha = p/C = 0.02$), the example storage is large for correlated patterns ($\alpha_s = s\alpha = 1.6$). On the right we display M for several values of α and large correlations ($b = 0.5$) such that we are in the G -phase. For increasing values of the threshold until $\theta = \theta_{opt}(\alpha)$ the overlap with a concept becomes larger indicating that the categorization ability improves. For $\theta > \theta_{opt}(\alpha)$ this categorization ability slowly decreases and at $\theta = \theta_Z(\alpha)$, the overlap M falls

abruptly to zero. This illustrates that for a very carefully tuned θ , $M \approx 1$, implying that categorization stays successful even for a concept loading larger than $\alpha = 3$. So compared with the categorization properties of the binary concept model (see Fig. 2 of [16]), we find that by using three-state concepts the categorization error is smaller and that a greater number of concepts can be categorized.

Next, an (α, θ) phase diagram is shown in Fig. 5. We take $A = 0.01$, $b = 0.5$ and a large number of examples $s = 80$ such that no R -phase appears. Categorization is then possible within the full line boundaries. Again the line G_{opt} indicates the values of $\theta(\alpha)$ for which M is maximal, thus E is minimal and hence the categorization is optimal. In the region between the full line and the (thick) dashed line, M is also of order 1, however Q is of the same order such that the condition for good categorization, $E < 0.1$, is not satisfied. Above the dashed-dotted line an S -phase does exist. Phase coexistence is possible in some regions and precisely what phase is attained depends on the initial conditions m_0^{11}, m_0^{1s} and Q_0 .

Finally, in Fig. 6 we show m and M as a function of θ for an analogue input-output relation $F_\theta = \tanh(x/\theta)$. For comparison, the same network parameters are used as in Fig. 4 for the three-state case and α again takes several values. Concerning retrieval of the examples a similar behaviour is found as in Fig. 4 with a slightly smaller m . Concerning categorization, however, although an analogous non-monotonous behaviour in θ is seen, M does not come close to 1 for larger α . It demonstrates that the gain parameter of a continuous input-output relation does not play the role the zero-activity threshold does for the three-state case. The reason is that in the three-state case this threshold switches of the neurons whose field h_i is not large enough such that the σ_i can match the three-state patterns ξ_i .

5. Concluding remarks

We have studied the retrieval and categorization properties of an extremely diluted three-state neural network through the solution of its parallel dynamics. In comparison with existing models in the literature the concepts are allowed to be three-state and the retrieval overlaps between the examples and the microscopic state of the network are not assumed to be fully symmetric. We find that the important parameters governing the transition from the retrieval to the categorization phase are the number of examples per concept

and their correlations. By choosing appropriately the zero-activity threshold of the neurons categorization can be considerably improved. In particular, in comparison with models for binary concepts the categorization error is smaller and a much greater number of concepts can be categorized.

Acknowledgments

We thank S.Amari, E.Koroutcheva, N.Parga and W.K.Theumann for useful discussions. This work has been supported in part by Cnpq/Brazil, the Universidad Autonoma de Madrid, and the Research Fund of the K.U.Leuven (grant OT/94/9). One of us (D.B.) is indebted to the Fund for Scientific Research - Flanders (Belgium) for financial support.

References

- [1] Parga N. and Virasoro M.A., *J. Phys. France* **47** (1986) 1857.
- [2] Feigelman M.V. and Ioffe L.B., *Int. J. Mod. Phys. B* **1** (1987) 51.
- [3] Bös S., Kühn R. and van Hemmen J.L., *Z. Phys. B* **71** (1988) 261.
- [4] Krogh A. and Hertz J.A., *J. Phys A: Math. Gen.* **21** (1988) 2211.
- [5] Gutfreund H., *Phys. Rev. A* **37** (1988) 570.
- [6] Fontanari J.F. and Meir R., *Phys. Rev. A* **40** (1989) 2806.
- [7] Fontanari J.F., *J. Phys. France* **51** (1990) 2421.
- [8] Miranda E., *J. Phys. I France* **I** (1991) 999.
- [9] Krebs P.R. and Theumann W.K., *J. Phys. A* **26** (1993) 3983.
- [10] Crisogono R., Tamarit A., Lemke N., Arenzon J. and Curado E., *J. Phys. A* **28** (1995) 1593.
- [11] Seung H.S., Sompolinsky H. and Tishby N., *Phys. Rev. A* **45** (1992) 6056.
- [12] Watkin T.L.H., Rau A. and Biehl M., *Rev. Mod. Phys.* **65** (1993) 499.

- [13] Engel A., *Mod. Phys. Lett. B* **8** (1994) 1683.
- [14] Oppen M. and Kinzel W., in *Physics of Neural Networks III*, eds. Doman E., van Hemmen J.L. and Schulten K. (Springer, 1996), p. 151.
- [15] Stariolo D.A., and Tamarit F.A., *Phys. Rev. A* **46** (1992) 5249.
- [16] Dominguez D.R.C. and Theumann W.K., *J. Phys. A* **29** (1996) 749.
- [17] Yedidia J.S., *J. Phys. A* **22** (1989) 2265.
- [18] Meunier C., Hansel D. and Verga A., *J. Stat. Phys.* **55** (1989) 859.
- [19] Derrida B., Gardner E., and Zippelius A., *Europhys. Lett.* **4** (1987) 167.
- [20] Bollé D., Vinck B., and Zagrebnov V.A., *J. Stat. Phys.* **70** (1993) 1099.
- [21] Bollé D., Shim G.M., Vinck B., and Zagrebnov V.A., *J. Stat. Phys.* **74** (1994) 565.
- [22] Bouten M., and Engel A., *Phys. Rev. E* **47** (1993) 139.

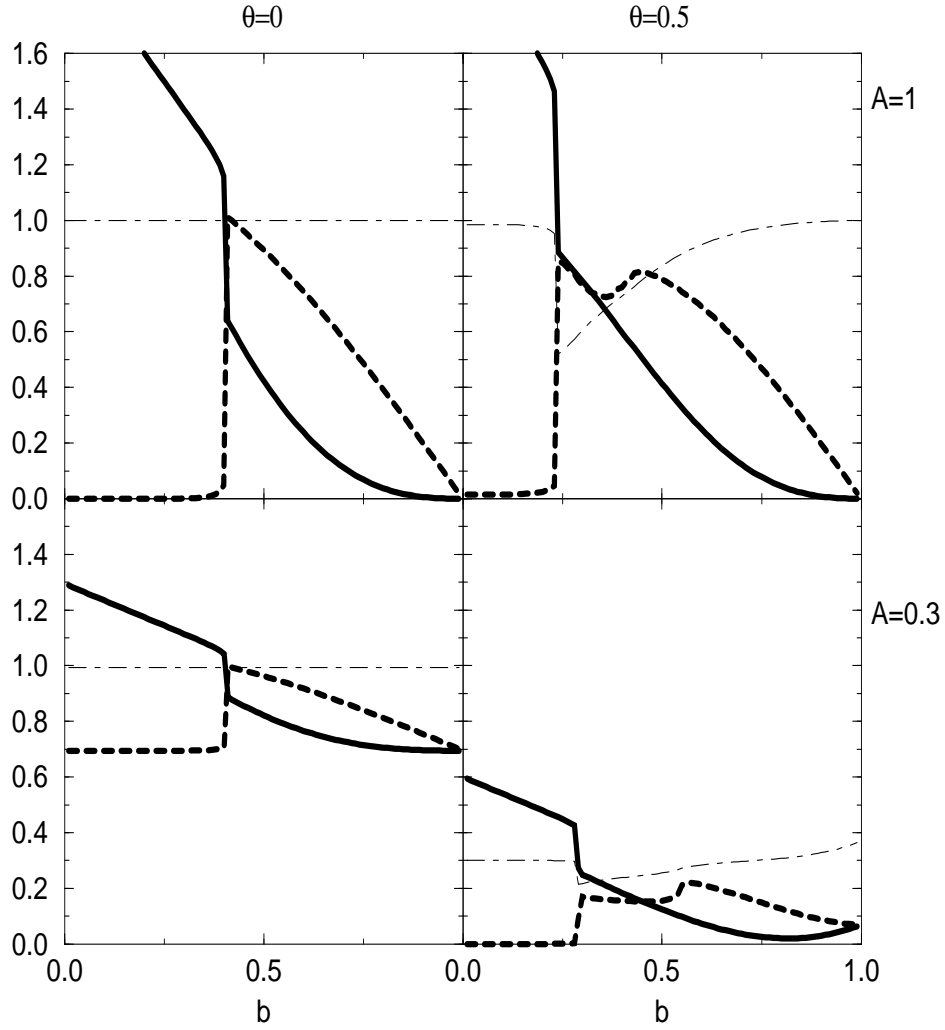


Figure 1: The Hamming distance D (dashed line), the categorization error E (full line) and the neuron activity Q (thin dashed-dotted line) as a function of the correlation b . The other network parameters are chosen as follows: the number of examples $s = 5$, the loading rate $\alpha = 0.01$, the activity $A = 1$ in the upper part and $A = 0.3$ in the lower part, and the zero-activity threshold $\theta = 0$ in the left part and $\theta = 0.5$ in the right part.

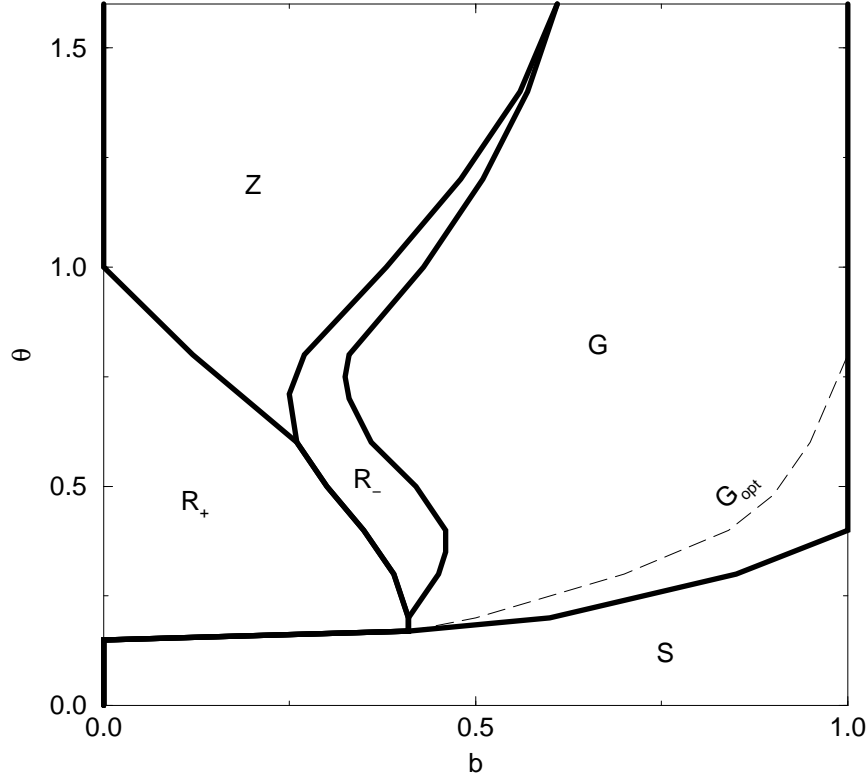


Figure 2: The (θ, b) phase diagram with $A = 0.1, s = 5$ and $\alpha = 0.01$. The following phases occur: the retrieval phases R_+ and R_- , the categorization phase G , the self-sustained activity phase S and the phase Z corresponding with the fixed-point zero. The thin dashed line G_{opt} indicates optimal categorization.

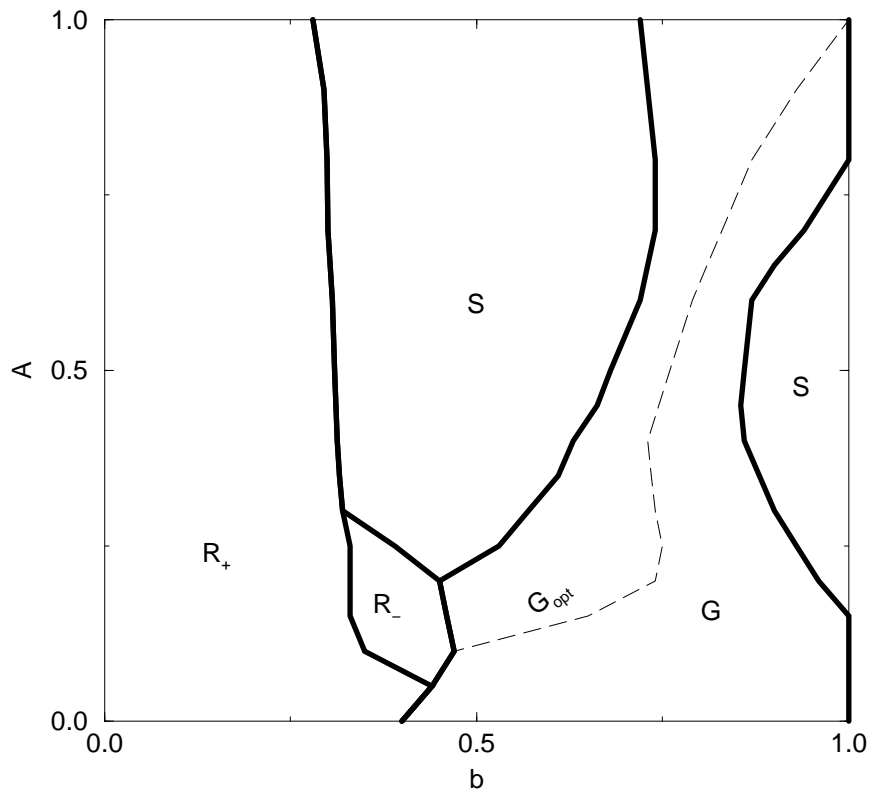


Figure 3: The (A, b) phase diagram with $\theta = 0.5, s = 5$ and $\alpha = 0.01$. The lines are as in Fig. 2.

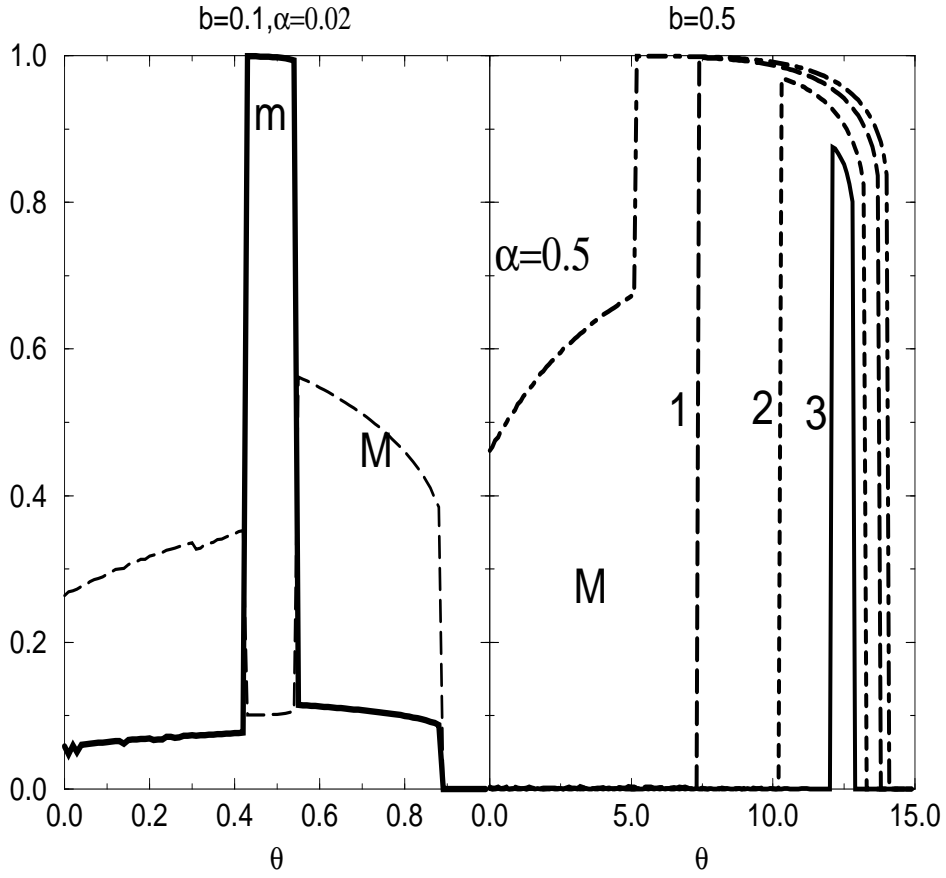


Figure 4: *Left : The overlaps m (full line) and M (dashed line) as a function of θ for $A = 0.01$, $s = 80$, $b = 0.1$ and $\alpha = 0.02$. Right : The overlap M as a function of θ for $A = 0.01$, $s = 80$, $b = 0.5$ and $\alpha = 0.5$ (dashed-dotted line), $\alpha = 1$ (dashed line), $\alpha = 2$ (dotted line) and $\alpha = 3$ (full line).*

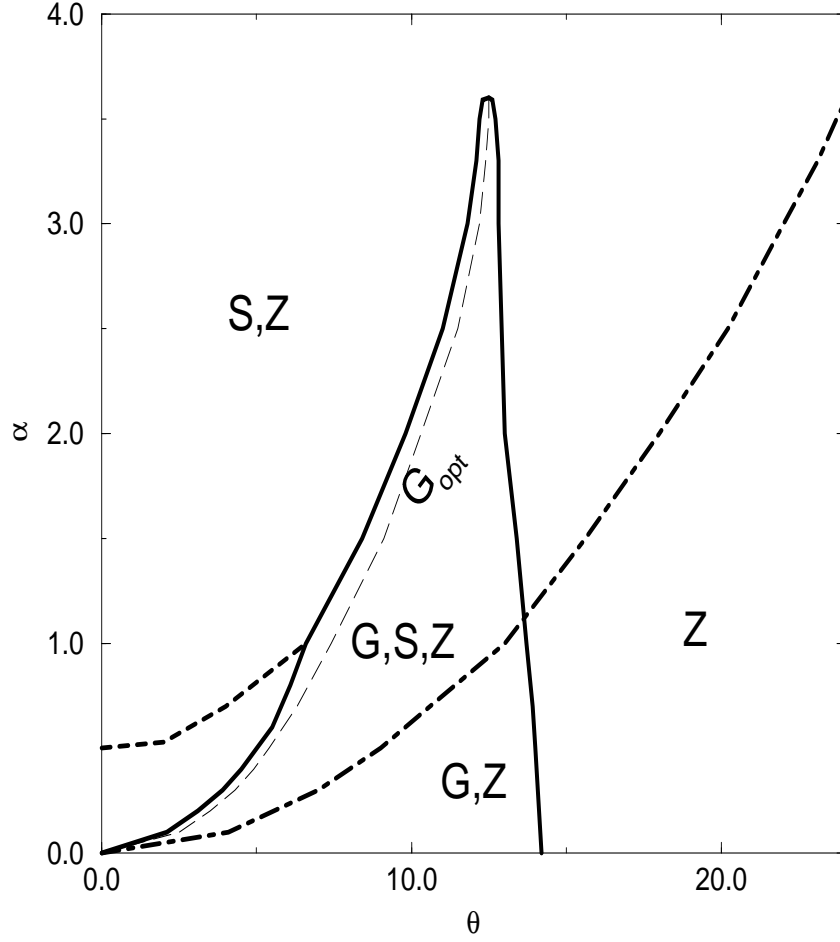


Figure 5: The (θ, α) phase diagram with $A = 0.01$, $s = 80$ and $b = 0.5$. Inside the full line the G -phase exists. Between the (thick) dashed line and the full line the condition $E < 0.1$ is not satisfied. Below the dashed-dotted line there exist no S -phase. The line G_{opt} is as in Fig. 2.

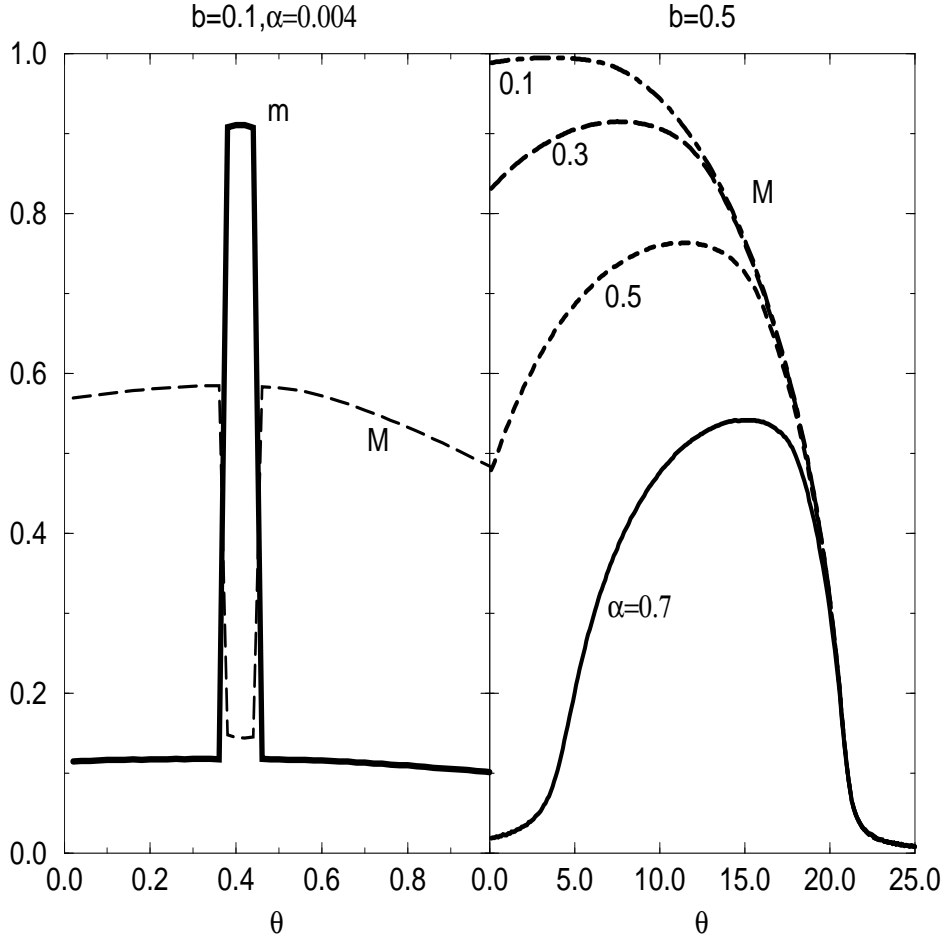


Figure 6: *Left* : The overlaps m (full line) and M (dashed line) as a function of θ for analogue neurons with $A = 0.01$, $s = 80$, $b = 0.5$ and $\alpha = 0.004$. *Right* : The overlap M as a function of θ for $A = 0.01$, $s = 80$, $b = 0.5$ and $\alpha = 0.1$ (dashed-dotted line), $\alpha = 0.3$ (dashed line), $\alpha = 0.5$ (dotted line) and $\alpha = 0.7$ (full line).